The Essential Role of Hydrogen-Bonding Interaction in the Extractive Separation of Phenolic Compounds by Ionic Liquid

Qiwei Yang, Huabin Xing, Baogen Su, Zongbi Bao, Jun Wang, Yiwen Yang, and Qilong Ren
Key Laboratory of Biomass Chemical Engineering, Ministry of Education, Dept. of Chemical and Biological Engineering, Zhejiang University, Hangzhou 310027, China

DOI 10.1002/aic.13939
Published online November 1, 2012 in Wiley Online Library (wileyonlinelibrary.com).

Separating phenols or even their homologs is an important process in environmental conservation and biomass utilization, and it has become one fascinating application of ionic liquids (ILs). Nevertheless, its underlying mechanism still needs to be elucidated at the molecular level. This work conducted a theoretical study on the interaction between ILs and phenols by quantum chemical calculations, using tocopherols as model compounds. Calculation results from geometry, electrostatic potential, natural bond orbital, atoms in molecules and energy analyses and their accordance with extraction experiments indicated the essential role of hydrogen-bonding interaction in extracting tocopherols and distinguishing the homologs by IL. The polarizable continuum model and conductor-like screening model for real solvents studies showed that the mechanism still holds when considering the solvation effect. Furthermore, with the aid of theoretical calculation, more efficient extractants, 1-ethyl-3-methylimidazolikum glycinate ([emim]Gly) and 1-ethyl-3-methylimidazolikum alaninate ([emim]Ala), were developed for the separation of tocopherol homologs. © 2012 American Institute of Chemical Engineers
AIChE J, 59: 1657–1667, 2013
Keywords: ionic liquid, extraction, biomass, separation techniques, computational chemistry (quantum chemistry)

Introduction

Ionic liquids (ILs) have attracted great attention as alternative extractants in liquid–liquid extraction in recent years, because of their unique properties such as structural and functional tunability, ultralow volatility, and low mutual solubility with water or weak-polar solvents.[1–5] Especially, ILs have shown notable efficiency on the extractive separation of phenolic compounds, which are one major class of the industrial chemicals and pollutants and are the most abundant bioactive compounds whose contents in biomass are only lower than cellulose, hemicellulose, and lignin.[6,7] ILs could selectively extract phenols from water or esters with elevated efficiency than common extractants.[8–15] Besides, IL-mediated extraction could also take effect in isolating a certain kind of phenolic compound from its structurally similar compounds or even homologs, which is a quite challenging task and common extractants just have very low separation selectivity,[16,17] with high efficiency. For example, we have utilized IL-mediated liquid–liquid extraction as a novel method for the separation of α-tocopherol, the major component of vitamin E,[18] from its homologs with selectivity higher than 20.0 (Figure 1).[19,20] Nevertheless, despite the promising experimental results obtained in the extractive separation of phenolic compounds by ILs, theoretical studies on the intermolecular interactions between phenolic compounds and ILs are quite few, how the ILs identify and extract phenols and even distinguish the minor difference of phenolic homologs is still not clearly illustrated at the molecular level. This situation leads to limited insight into the underlying extraction mechanism and limitation on the development of new extractants. Different from common molecular solvents, ILs are "two-component" solvents consisted of cations and anions, so they usually contain multiple functional groups in their structures.[21] These functional groups, including hydrogen-bond acceptor and donor sites, aromatic ring, and weak-polar aliphatic chains, can make the interaction between ILs and phenolic compounds complicated; thus, a theoretical study on the interaction is indeed necessary and has to be improved.

In this work, a theoretical study has been conducted on the intermolecular interaction between ILs and tocopherols by quantum chemical calculations, where tocopherols are selected as a model of phenolic compounds because their structures are relatively complicated than common phenols, and the separation of tocopherol homologs is a quite challenging process. Atoms in molecules (AIM) and natural bond orbital (NBO) analysis were used to give more insight into the features of intermolecular interactions besides the general geometry and energy analysis. Calculation results were discussed together with the comparison to extraction experiments, and then an attempt to develop more efficient IL extractants was carried out.

Calculation Details

The geometry optimization calculations in the gas phase were performed on isolated tocopherol molecules, ion pairs, and their complexes, using Gaussian 03 software.[22] The

Additional Supporting Information may be found in the online version of this article.

Correspondence concerning this article should be addressed to Q. Ren at renql@zju.edu.cn or H. Xing at xinghb@zju.edu.cn.

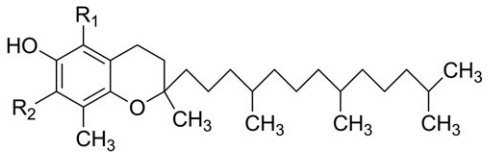

Compound	R_1	R_2
α-Tocopherol	$-CH_3$	$-CH_3$
β-Tocopherol	$-CH_3$	$-H$
γ-Tocopherol	$-H$	$-CH_3$
δ-Tocopherol	$-H$	$-H$

Figure 1. The structure of tocopherols.

hybrid density functional theory (DFT) that incorporates Becke's three-parameter exchange with Lee, Yang, and Parr's (B3LYP) correlation functional method and the 6-31+G(d,p) basis set were employed.[23,24] Due to the large size of these molecules containing atoms more than 100, the initial geometries of tocopherols were constructed and preoptimized at the semiempirical level with the Chem3D Ultra package,[25] and then the obtained geometry having the lowest energy was further optimized with the Gaussian 03 software. The optimization of ion pair was directly performed with the Gaussian 03 software. For each kind of ion pair, more than five different initial geometries were optimized, where the anion was located at different positions around the cation. The optimized geometry having the lowest energy was used as the global minimum for the subsequent calculation. All the optimized structures were confirmed to be minima on the potential energy surface via vibrational frequency analysis. It should be stated that due to the flexibility of the long alkyl chain, it would be difficult to confirm whether the real global minimum of the potential energy surface of tocopherol is found. Nevertheless, considering that the focus of this work is the hydrogen-bonding interaction of the phenolic hydroxyl group of tocopherols with ILs and that the hydrogen-bond donor ability of the phenolic hydroxyl is not likely to be susceptible to the conformation of the alkyl side chain, the geometry diversity of tocopherols resulting from the flexible alkyl chain should not have a significant impact on the subsequent calculation.

Besides the geometry parameters and electrostatic potentials, NBO and AIM analysis were also performed for the optimized structures to give an insight into the intermolecular interactions.[26–29] NBO analysis was performed at the B3LYP/6-31+G(d, p) level by the NBO 3.1 program as implemented in the Gaussian 03 package of programs, and AIM analysis was performed using the AIMAll software.[30] The interaction energy between ion pair and tocopherol (ΔE) was calculated with the correction for the basis set superposition error (BSSE) by the counterpoise method.[31]

The single-point calculation and optimization within an implicit solvent media of the optimized structures of tocopherols, IL pairs, and IL–tocopherol complexes in the gas phase were performed using the integral equation formulation of the polarizable continuum model (PCM) as implemented in the Gaussian 03 software at the B3LYP/6-31+G(d,p) level.[32] The corresponding United Atom Topological Model applied on radii optimized for the HF/6-31G(d) level of theory (UAHF) atomic radii were used to build the solute cavities, and the values of RMin and OFac parameters were set to 0.5 and 0.8, respectively. The default solvent used in the calculations was dimethyl sulfoxide, because it is perhaps the closest to an IL solvent in polarity among the standard solvents in Gaussian 03. The dielectric constants (ε) of ILs were obtained from the literature.[33] The molar volumes (V_{mol}) and the solvent particle density (N) could be determined by the molecular weight and density of the specific IL.[33] The radius of the solvent molecule (R_{solv}) was estimated based on the molar volume of the IL assuming a hard sphere model.[34] The ionic strength (I) of IL was calculated assuming complete dissociation of the ion pairs, which was not necessarily true. Table 1 lists the various parameters of the ILs used in Gaussian 03 for solvation calculations. Because it is not possible in Gaussian 03 to perform calculations using both the counterpoise correction and an implicit solvation method, the gas-phase BSSE energy of the solvated geometry of IL and IL–tocopherol complex was used to correct the corresponding interaction energy.

The conductor-like screening model for real solvents (COSMO-RS) calculation was performed with the COSMOthermX program.[35] The required COSMO polarization charge densities σ of the molecular surfaces were computed by the TURBOMOLE 6.3 program package on the density functional theory level,[36] utilizing the B-P86 functional with resolution of identity approximation and a triple-ζ valence polarized basis set.[37–39] The optimized geometries of isolated IL pairs and tocopherols in the gas phase with Gaussian 03 were used as starting structures for the calculation in TURBOMOLE 6.3.

Experimental Method

Chemicals

1-Ethyl-3-methyl bromide ([emim]Br, 99%) and glycine (99.5%) were purchased from Green Chemistry and Catalysis, LICP, CAS (China) and Aladdin Chemical (China), respectively. 1-Ethyl-3-methyl acetate ([emim]Ac, 99%) was purchased from Chengjie Chemical (China). The mixed tocopherols (99%) were supplied by Heilongjiang Jiusan Oil and Fat (China), which were produced from soybean deodorizer distillate, containing 45.3% δ-tocopherol, 44.5% $\beta\gamma$-tocopherol, and 9.1% α-tocopherol. All other chemicals (analytical grade) were commercially available and used as received unless otherwise stated.

Synthesis of [emim]Gly and [emim]Ala

The amino acid functionalized ILs 1-ethyl-3-methylimidazolium glycinate ([emim]Gly) containing glycine anion and 1-ethyl-3-methylimidazolium alaninate ([emim]Ala) containing alaninate anion were synthesized with a two-step procedure according to the previous literature.[40,41] The first step

Table 1. The Solvent Properties of ILs Used for the Solvation Calculations by Gaussian 03

IL	ρ (g cm^{-3})	M_w	V_{mol} (cm^{-3})	R_{solv} (Å)	Number Density (Particle Å^{-3})	I (mol dm^{-3})	ε
[bmim]Cl	1.0820	174.67	161.4	3.2237	0.00373	6.196	15.0
[bmim]BF_4	1.2141	226.02	186.2	3.3810	0.00323	5.371	12.0

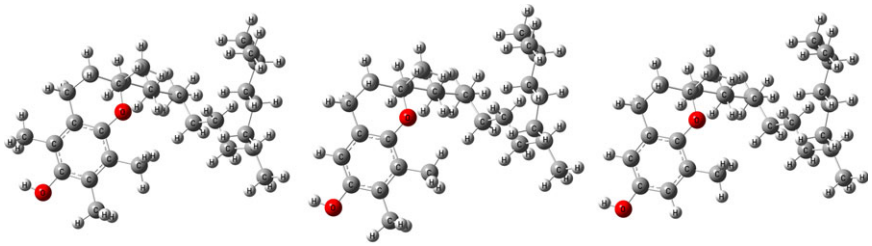

a) α-tocopherol b) γ-tocopherol c) δ-tocopherol

Figure 2. Optimized structures of tocopherols at B3LYP/6-31+G(d,p) level.

[Color figure can be viewed in the online issue, which is available at wileyonlinelibrary.com.]

was the anion-exchange reaction of [emim]Br to [emim]OH over a column packed with strongly basic anion-exchange resin along with the common $AgNO_3$ test on the elution. The second step was the neutralization reaction between [emim]OH aqueous solution and excessive amino acid. After the purification, the purity of synthesized ILs was confirmed by ^{1}H NMR analysis. The ^{1}H NMR results agreed well with those reported by other researchers.[41] The water mass fraction of [emim]Gly, [emim]Ala, and [emim]Ac were 0.62, 0.67, and 0.36%, respectively, determined by the Karl-Fischer titration after heating under vacuum for about 36 h.

Extraction

The extraction experiments were performed as described elsewhere.[20] Typically, a known amount of the mixed tocopherols was dissolved in hexane, and aliquots of this solution were contacted with an equal volume of a IL–acetonitrile mixture in an Erlenmeyer flask. The flask was shaken for 2 h using a thermostatic rotary shaker with a speed of 200 r min^{-1} and then settled at the same temperature to reach a phase splitting. Samples were taken from each of the two phases and diluted with the mixture of methanol and water (96/4, v/v) for the high-performance liquid chromatography (HPLC) analysis. The HPLC systems consisted of an autosampler, an Atlantis C18 column (5 μm, 4.6 $\times$ 250 mm^2), a Waters 1525 binary pump, and a Waters 2487 dual λ absorbance detector. The mobile phase was a mixture of methanol and water (96/4, v/v). The detection of tocopherols was performed at 292 nm. β-Tocopherol and γ-tocopherol were measured as a combined fraction, because their structures are so similar that their HPLC peaks were overlapped under the analytical condition. The extraction equilibrium experiments were repeated for three times, and the relative uncertainties of distribution coefficient were within 5%. The distribution coefficient of tocopherol was calculated by the following equation

$$D_i = C_i^{\mathrm{e}}/C_i^{\mathrm{r}}$$

where C_i^{e} and C_i^{r} refer to the mass fractions of solute i in the extract phase (IL-rich phase) and in the raffinate phase (hexane-rich phase), respectively.

Results and Discussion

Calculation on tocopherols

The optimized structures of three tocopherol homologs, α-tocopherol, γ-tocopherol, and δ-tocopherol, are shown in Figure 2, which seem very similar. The electrostatic potential surfaces for those structures are constructed and shown in Figure 3, where the red and blue colors indicate the negative and positive regions, respectively. It is found that most regions around the molecules are nearly neutral except the regions near the two oxygen atoms and the phenolic hydrogen atom. This indicates that the phenolic hydroxyl group is the main possible region of tocopherols to interact with other molecules via specific interactions. The phenolic hydrogen that possesses strong positive electrostatic potential values is likely the main site to be attacked by the nucleophilic sites of other molecules.

Platts[42] has found that the value of the electrostatic potential at the hydrogen-bond donor hydrogen nuclear position (excluding the hydrogen's own infinite nuclear contribution), EP_{nuc}, showed a good correlation with the hydrogen-bond donor capacity of the molecules. The larger EP_{nuc} values tended to result in stronger hydrogen-bond donor capacity. The EP_{nuc} values of tocopherol homologs based on the optimized structures were calculated to clarify the difference of the property of homologs. The obtained values decrease in the order δ-tocopherol (-0.978) > γ-tocopherol (-0.979) >

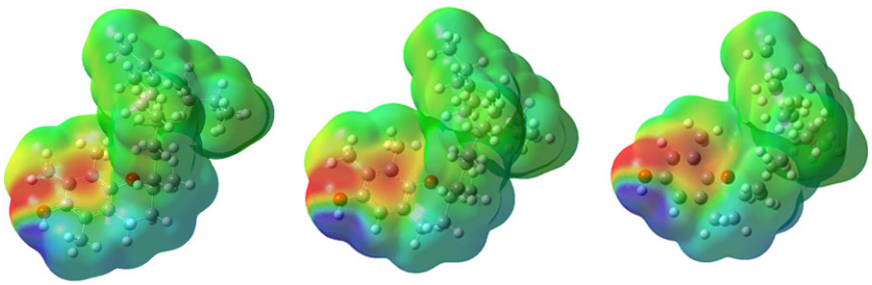

a) α-tocopherol b) γ-tocopherol c) δ-tocopherol

Figure 3. B3LYP/6-31+G(d,p) electrostatic potential mapped onto the 0.0004 density isosurface (unit: electron bohr^{-3}) for the optimized structures of tocopherols.

The scale spans -15.7 (red) through 0.0 (green) to 15.7 (blue) (unit: kcal mol^{-1}). [Color figure can be viewed in the online issue, which is available at wileyonlinelibrary.com.]

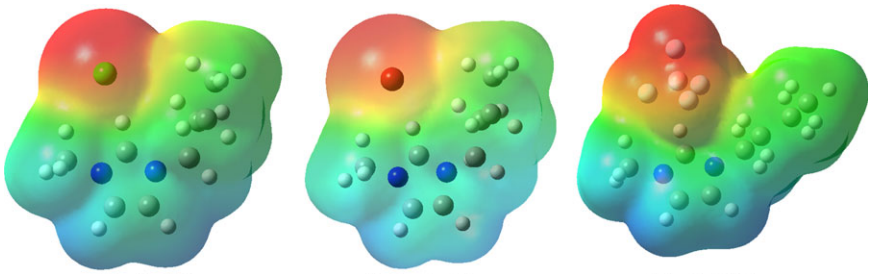

Figure 4. B3LYP/6-31+G(d,p) electrostatic potential mapped onto the 0.0004 density isosurface (unit: electron bohr^{-3}) for the optimized structures of [bmim]Cl, [bmim]Br, and [bmim]BF_4.

The scale spans −50.2 (red) through 0.0 (green) to 50.2 (blue) (unit: kcal mol^{-1}). [Color figure can be viewed in the online issue, which is available at wileyonlinelibrary.com.]

α-tocopherol (−0.982). This order probably indicates that δ-tocopherol has the strongest hydrogen bond capacity among the homologs and α-tocopherol has the weakest.

Calculation on ILs

Optimized structures were obtained for three common ILs, 1-butyl-3-methylimidazolium chloride ([bmim]Cl), 1-butyl-3-methylimidazolium bromide ([bmim]Br), and 1-butyl-3-methylimidazolium tetrafluoroborate ([bmim]BF_4). These ILs have ever been used as extractant for the extractive separation of tocopherol homologs in our previous work. As shown in Figure 4, the location of anions shows obvious preference on the region near the C_2—H group (C_2 is the carbon atom between the two nitrogen atoms) of cation in all cases. This preference has been observed in many kinds of ILs as a result of the relatively strong interaction between C_2—H and anions.[43,44] The electrostatic potential surfaces were also constructed for ILs. As also shown in Figure 4, there is a strong negative region near the anions and the electrostatic potential around the cation is nearly neutral or weak positive. It indicates that those ILs are likely to have specific interactions with the positive sites of other molecules,[45] such as the hydrogen atom of phenolic hydroxyl group in tocopherols, through their anions.

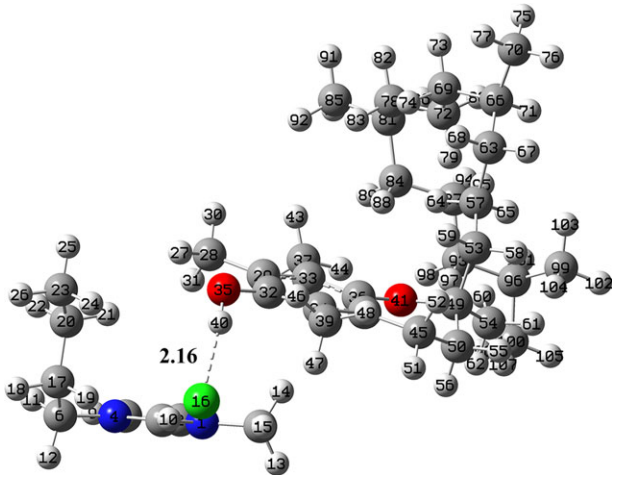

Figure 5. Optimized structure of [bmim]Cl-α-tocopherol complex at B3LYP/6-31+G(d,p) level.

Dashed line implies hydrogen bond, with a decimal showing the distance (unit: Å). [Color figure can be viewed in the online issue, which is available at wileyonlinelibrary.com.]

Hydrogen-bonding interaction between IL and tocopherol

The above electrostatic potential analysis indicates that specific interaction of IL with tocopherols is likely to exist between the anion and the hydroxyl group. Therefore, optimized structures where the anion lies near the hydroxyl group were obtained for ion pair-tocopherol 1:1 complexes. The sum of van der Waals atomic radii of two atoms was often used as a criterion in geometry analysis to judge if a hydrogen bond is present between one covalently bonded hydrogen and other electronegative atoms.[46] In the optimized [bmim]Cl-α-tocopherol complex (Figure 5), the $Cl_{16}\cdots H_{40}$ distance in $Cl_{16}\cdots H_{40}$—O_{35} is 2.16 Å, much smaller than the sum of van der Waals atomic radii of hydrogen and chloride (2.95 Å),[47] implying the presence of one intermolecular $Cl_{16}\cdots H_{40}$—O_{35} hydrogen bond between the anion and the phenolic hydroxyl group. This agrees with the electrostatic potential distribution discussed earlier that the hydroxyl hydrogen of tocopherol possesses strong positive electrostatic potential, and there is a strong negative electrostatic potential region near the anion of IL. The $Cl_{16}\cdots H_{47}$ distance in $Cl_{16}\cdots H_{47}$—C_{39} is 2.95 Å, just around the critical value, so it seems hard to judge whether a hydrogen bond is present in $Cl_{16}\cdots H_{47}$—C_{39}. AIM analysis on the optimized geometry was performed to obtain more insight to the intermolecular interaction between [bmim]Cl and α-tocopherol. Three intermolecular bond critical points (BCPs) in the [bmim]Cl-α-tocopherol complex were identified from the AIM analysis, $Cl_{16}\cdots H_{40}$, $Cl_{16}\cdots H_{47}$, and $O_{35}\cdots H_{21}$. The hydrogen-bonding criteria proposed by Popelier within the AIM theoretical frame were used to analyze whether these BCPs relate to intermolecular hydrogen bonds.[48,49] Consequently, it was found that a hydrogen bond existed in $Cl_{16}\cdots H_{40}$—O_{35}. As presented in Table 2, the charge density evaluated at the BCP, ρ_c, of $Cl_{16}\cdots H_{40}$ is 0.0280 au, within the criterion that ρ_c should be between 0.002 and 0.035 au; the value of the Laplacian of ρ_c, $\nabla^2\rho_c$, is 0.0590 au, within the criterion that $\nabla^2\rho_c$ should be between 0.024 and 0.139 au. Nevertheless, the other two BCPs probably do not relate to notable hydrogen bonds or just relate to very weak hydrogen bonds due to their much lower ρ_c and $\nabla^2\rho_c$ values. ρ_c is an useful parameter for estimating the relative strength of corresponding bond,[26,50] so the hydrogen bond $Cl_{16}\cdots H_{40}$—O_{35} is known much stronger than the interaction within $Cl_{16}\cdots H_{47}$ and $O_{35}\cdots H_{21}$ due to its much higher ρ_c value. In addition, the total energy density at BCP, H_c, of $Cl_{16}\cdots H_{40}$ is negative and those of $Cl_{16}\cdots H_{47}$ and $O_{35}\cdots H_{21}$ are positive, also

Table 2. Charge Density ρ_c, Its Laplacian $\nabla^2\rho_c$, Energy Density H_c at the BCP from AIM Analysis, Second-Order Stabilization Energy $E^{(2)}$ from NBO Analysis, and the BSSE-Corrected Interaction Energy ΔE of IL-α-Tocopherol Complex at B3LYP/6-31+G (d,p) Level

IL	BCP	$\rho_c \times 10^2$ (au)	$\nabla^2\rho_c \times 10^2$ (au)	$H_c \times 10^3$ (au)	Electron Delocalization	$E^{(2)}$ (kcal mol^{-1})	ΔE (kJ mol^{-1})
[bmim]Cl	$Cl_{16}\cdots H_{40}$	2.80	5.90	−1.5	LP Cl_{16}–BD* O_{35}—H_{40}	23.11	−45.17
	$Cl_{16}\cdots H_{47}$	0.69	2.29	1.3	LP Cl_{16}–BD* C_{39}—H_{47}	1.04	
	$O_{35}\cdots H_{21}$	0.30	1.12	0.7	LP O_{35}–BD* C_{20}—H_{21}	0.17	
[bmim]Br	$Br_{107}\cdots H_{30}$	2.49	4.85	−1.0	LP Br_{107}–BD* O_7—H_{30}	20.71	−38.05
[bmim]BF_4	$F_{91}\cdots H_{15}$	2.46	8.02	−0.7	LP F_{91}–BD* O_{12}—H_{15}	12.50	−23.60

indicating that the hydrogen bond $Cl_{16}\cdots H_{40}$—O_{35} is much stronger than the interaction within $Cl_{16}\cdots H_{47}$ and $O_{35}\cdots H_{21}$. It is known that bonds with any degree of covalent character must have a negative H_c, which is less than zero.[51,52] Thus, the hydrogen bond $Cl_{16}\cdots H_{40}$—O_{35} has partially covalent character and, consequentially, stronger than the other two interactions that just appear to represent purely electrostatic interactions. The second-order perturbation theory analysis of Fock matrix in NBO basis was further performed to know more about the interactions.[29] All possible interactions between "filled" (donor) Lewis-type NBOs and "empty" (acceptor) non-Lewis NBOs can be examined by estimating their energetic importance with second-order perturbation theory. The second-order stabilization energy of each donor–acceptor interaction, $E^{(2)}$, is useful for judging the interaction strength.[53] In the investigated [bmim]Cl-α-tocopherol complex, the dominant donor–acceptor interaction is the $n_{Cl} \rightarrow \sigma^*_{OH}$ interaction between the filled lone pair of chloride anion and the antibond of hydroxyl group, which has much higher stabilization energies than other donor–acceptor interactions. The stabilization energy of LP Cl_{16}–BD* O_{35}—H_{40} interaction is 23.11 kcal mol^{-1}, but the sum of the stabilization energy of all the other intermolecular donor–acceptor interactions (above the output threshold 0.05 kcal mol^{-1}) is less than 4.0 kcal mol^{-1}. Thus, the significance of anion-hydroxyl hydrogen-bonding interaction is illustrated. It was reported that the $E^{(2)}$ values of LP (O) → BD* (OH) interaction between phenol and several kinds of hydrogen-bond acceptor molecules, including acetone, methanol, and water, were all lower than 12 kcal mol^{-1},[54] so the [bmim]Cl seems having a relatively strong hydrogen-bond acceptor capacity.

Quantum chemical calculations on the interaction between [bmim]Br or [bmim]BF_4 and α-tocopherol were further carried out. [bmim]Br and [bmim]BF_4 contain the same cation with [bmim]Cl and differ in the kind of anion. From the optimized geometries where the anion lies near the hydroxyl group, intermolecular hydrogen bonds were identified according to the van der Waals radius criterion. Especially, obvious hydrogen bonds were found between the anion of IL (bromide or fluorine atom) and the hydroxyl group (Figure 6). These hydrogen bonds were further identified by the Popelier's criterion within AIM theory. The ρ_c of $Br_{107}\cdots H_{30}$ is 0.0249 au in [bmim]Br-α-tocopherol complex, and the ρ_c of $F_{91}\cdots H_{15}$ is 0.0246 au in [bmim]BF_4-α-tocopherol complex (Table 2). The second-order stabilization energy of the interaction between the lone pair of bromide and the antibond of hydroxyl group of tocopherol is 20.71 kcal mol^{-1} in [bmim]Br-α-tocopherol complex and that of the interaction between the lone pair of fluoride and the antibond of hydroxyl group of tocopherol is 12.50 kcal mol^{-1} in [bmim]BF_4-α-tocopherol complex.

Comparing the calculation results on different IL-α-tocopherol complexes, it could be found that the ρ_c and $E^{(2)}$ values between IL and α-tocopherol all followed the order [bmim]Cl > [bmim]Br > [bmim]BF_4. Because the higher ρ_c and $E^{(2)}$ values relate to stronger intermolecular hydrogen-bonding interaction, the interaction strength of [bmim]Cl with tocopherols is considered stronger than [bmim]Br and [bmim]BF_4. Moreover, when comparing the BSSE-corrected interaction energy ΔE between α-tocopherol and different ILs, the order was found to be also [bmim]Cl > [bmim]Br > [bmim]BF_4 (a higher ΔE refers to a more negative value), implying the relative interaction strength of different ILs again. This result is consistent with the experimental distribution coefficients of α-tocopherol in different IL-based biphasic systems. Although in the experiments the used extractant was IL–cosolvent mixture rather than pure IL, the primary role of IL in the extraction has been revealed by the

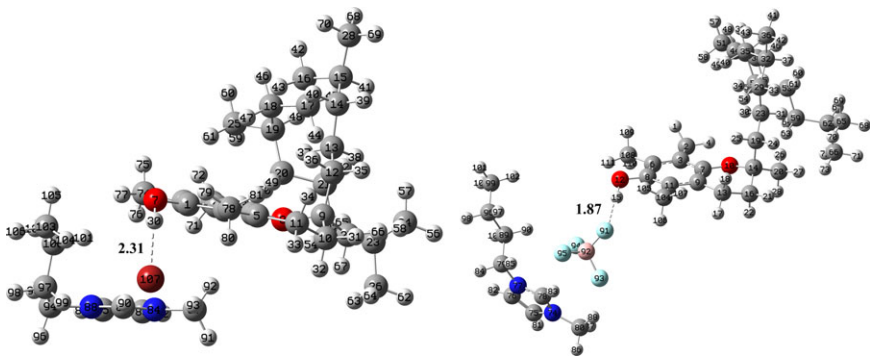

Figure 6. Optimized structure of [bmim]Br-α-tocopherol (left) and [bmim]BF_4-α-tocopherol (right) complexes at B3LYP/6-31+G(d,p) level.

Dashed lines imply hydrogen bonds, with decimals showing the distances (unit: Å). [Color figure can be viewed in the online issue, which is available at wileyonlinelibrary.com.]

Table 3. Extractive Separation of Tocopherol Homologs Using Different IL-Acetonitrile Mixtures at 303.15 K*

	Distribution Coefficient			Selectivity	
IL	δ	$\beta\&\gamma$	α	δ/α	$\beta\&\gamma/\alpha$
[bmim]BF_4[19]	0.30	0.18	0.09	3.3	2.0
[bmim]Br[19]	1.23	0.69	0.18	6.8	3.8
[bmim]Cl[19]	3.54	1.94	0.37	9.6	5.2
[emim]Gly	19.2	9.31	1.51	12.7	6.2
[emim]Ala	20.9	10.5	1.55	13.5	6.8
[emim]Ac	19.3	9.40	1.39	13.9	6.8

*The initial concentration of tocopherol in hexane (mg cm^{-3}): δ 1.00, $\beta\&\gamma$ 0.98, and α 0.20. Molar ratio of IL to acetonitrile: 2:98.

experiments, and the variation of distribution equilibrium against different mixtures can be approximately regarded as against different ILs. As shown in Table 3, the distribution coefficient of α-tocopherol in [bmim]Cl-based system is the largest and that in [bmim]BF_4 is the smallest, implying the stronger intermolecular interaction of α-tocopherol with [bmim]Cl than with [bmim]Br and even more [bmim]BF_4.

The interaction between ILs and δ-tocopherol was also investigated by DFT calculation, and similar results with the case of α-tocopherol were found. The anion of IL could interact with δ-tocopherol by forming X···H—O hydrogen bonds, and the analysis from the ρ_c, $E^{(2)}$, and ΔE exhibits the magnitude of hydrogen bond between tocopherol and different ILs is also in the order [bmim]Cl > [bmim]Br > [bmim]BF_4. This result is consistent with the experimental distribution coefficients of δ-tocopherol in different IL-based biphasic systems (Table 3).

Interaction with different tocopherol homologs

Why the ILs can recognize the tiny structural difference of tocopherol homologs in liquid–liquid extraction is very interesting. As an attempt to resolve this problem, calculation results were compared for the [bmim]Cl-tocopherol complexes (Tables 2 and 4, Figure 7). From AIM analysis, the charge density evaluated at the BCP, ρ_c, of $Cl\cdots H_{O—H}$ is 0.0324 au for [bmim]Cl-δ-tocopherol, 0.0318 au for [bmim]Cl-γ-tocopherol, and 0.0280 au for [bmim]Cl-α-tocopherol, respectively, following the order δ-tocopherol > γ-tocopherol > α-tocopherol. From NBO analysis, the second-order stabilization energy, $E^{(2)}$, of LP Cl → BD* O—H donor–acceptor interaction is 26.54 kcal mol^{-1} for [bmim]Cl-δ-tocopherol, 25.72 kcal mol^{-1} for [bmim]Cl-γ-tocopherol, and 23.11 kcal mol^{-1} for [bmim]Cl-α-tocopherol, respectively, also following the order δ-tocopherol > γ-tocopherol > α-tocopherol. Furthermore, the BSSE-corrected interaction energy ΔE between [bmim]Cl and tocopherols has the same order, δ-tocopherol (54.63 kJ mol^{-1}) > γ-tocopherol (53.25 kJ mol^{-1}) > α-tocopherol (45.17 kJ mol^{-1}). These results show that the intensity of hydrogen-bonding interaction between anion and hydroxyl group is different for each tocopherol homolog, so [bmim]Cl could selectively interact with different homologs and have the capacity to separate them experimentally. In more detail, the calculation shows that the interaction between [bmim]Cl and δ-tocopherol is the strongest whereas the interaction between [bmim]Cl and α-tocopherol is the weakest, and the difference between [bmim]Cl-δ-tocopherol and [bmim]Cl-γ-tocopherol is relatively small and their difference with [bmim]Cl-α-tocopherol is much larger. Thus, in a separation experiment, the δ-tocopherol is most likely to be attracted by [bmim]Cl, with slightly weaker affinity of γ-tocopherol but much weaker affinity of α-tocopherol to [bmim]Cl. As shown in Table 3, when using [bmim]Cl as extractant in extraction experiments, the distribution coefficients of tocopherols are just in the order δ-tocopherol > γ-tocopherol > α-tocopherol, and in more detail, the difference of distribution coefficients between δ-tocopherol and γ-tocopherol is relatively small and the difference between δ-/γ-tocopherols and α-tocopherol is much larger. Thus, the calculation results are in good accordance with the experiments, and it implies that the hydrogen-bonding interaction between anion and hydroxyl group plays an essential role in the selective extraction of different tocopherol homologs.

Investigation on the interaction between [bmim]Br/[bmim]BF_4 and different tocopherol homologs exhibits the same results with the [bmim]Cl-tocopherol interaction described earlier. The ρ_c, $E^{(2)}$, and ΔE values of [bmim]Br/[bmim]BF_4-δ-tocopherol complexes are higher than [bmim]Br/[bmim]BF_4-α-tocopherol complexes (Table 4), in accordance with the experimental result that δ-tocopherol has a much higher distribution coefficient than α-tocopherol when using [bmim]Br and [bmim]BF_4 as extractant. Thus, the essential role of hydrogen-bonding interaction between anion and hydroxyl group in the selective extraction of different tocopherol homologs is further demonstrated.

Multiple interactions between IL and tocopherol

The essential role of hydrogen-bonding interaction between anion and hydroxyl group in the extraction of tocopherols has been demonstrated in the above discussion. Besides the hydrogen bond, intermolecular p–π and σ–π interactions were also found by taking more insight into the DFT calculation results on IL–tocopherol complexes. For example, in the NBO analysis for [bmim]Cl-δ-tocopherol, it is found that there is a donor–acceptor interaction between the lone pair of hydroxyl oxygen atom and the second antibond of C—N bond in the imidazolium ring of cation (Table 5). Further investigation on the composition of the corresponding two NBOs shows that the antibond of C—N bond mainly consists of the p orbitals of the two atoms and the lone pair of hydroxyl oxygen nearly consists of its p orbital, so the donor–acceptor interaction is recognized as a p–π interaction. Nevertheless, the $E^{(2)}$ value of this interaction is much smaller than the LP Cl → BD* O—H donor–acceptor interaction, implying a weaker strength than the anion-hydroxyl hydrogen-bonding interaction. Other typical p–π

Table 4. Charge Density ρ_c, Its Laplacian $\nabla^2\rho_c$, Energy Density H_c at the BCP from AIM Analysis and Second-Order Stabilization Energy $E^{(2)}$ from NBO Analysis of the anion-hydroxyl hydrogen-bonding interaction, and the BSSE-Corrected Interaction Energy ΔE of IL–Tocopherol Complex at B3LYP/6-31+G (d,p) Level

Complex	$\rho_c \times 10^2$ (au)	$\nabla^2\rho_c \times 10^2$ (au)	$H_c \times 10^3$ (au)	$E^{(2)}$ (kcal mol^{-1})	ΔE (kJ mol^{-1})
[bmim]Cl-γ-tocopherol	3.18	6.38	−2.4	25.72	−53.25
[bmim]Cl-δ-tocopherol	3.24	6.42	−2.5	26.54	−54.63
[bmim]Br-δ-tocopherol	2.64	4.96	−1.3	21.94	−46.33
[bmim]BF_4-δ-tocopherol	2.58	8.25	−0.8	13.03	−29.21

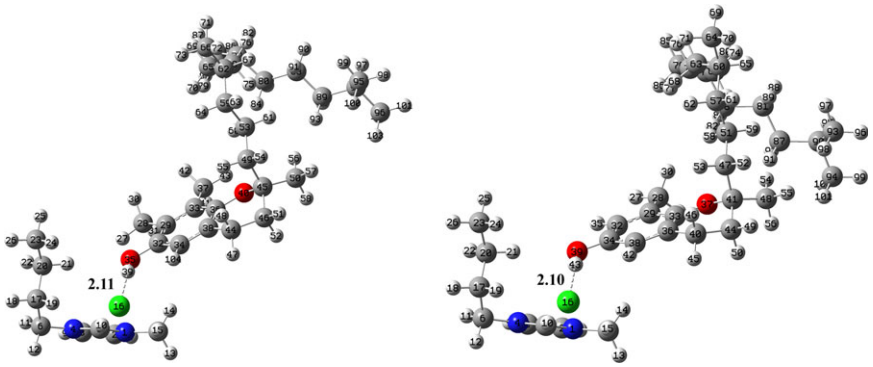

Figure 7. Optimized structure of [bmim]Cl-γ-tocopherol (left) and [bmim]Cl-δ-tocopherol (right) complexes at B3LYP/6-31+G(d,p) level.

Dashed lines imply hydrogen bonds, with decimals showing the distances (unit: Å). [Color figure can be viewed in the online issue, which is available at wileyonlinelibrary.com.]

and σ–π donor–acceptor interactions are also listed in Table 5, and all of them have small $E^{(2)}$ values. Considering that nonspecific van der Waals intermolecular interactions certainly exist between IL and tocopherol, multiple interactions including hydrogen bond, p–π, σ–π, and van der Waals interactions have been found between ILs and tocopherols. ILs are two-component solvents consisting of both cation and anion, so multiple functional groups can exist in their structures that cause the capacity of ILs to have multiple interactions with other molecules.

Solvation effects on IL–tocopherol interactions

Although the above gas-phase calculations showed a good relationship between the IL–tocopherol hydrogen-bonding interaction and the extractive separation of tocopherols by ILs, it will be useful to investigate the effect of solvation on calculation results to see if the relationship still holds with increased realism of calculation.[55] Considering the large size of calculated structures in this work, implicit solvation approach using a PCM by Gaussian 03 software was used, for the interaction between two ILs ([bmim]Cl, [bmim]BF_4) and two tocopherol homologs (α-/δ-tocopherol). Two different strategies were investigated for the calculation. In the first strategy, the single-point calculation within the implicit solvent was directly performed on the optimized gas-phase structures, which was widely used in previous literature.[56,57] As shown in Table 6, although the interaction strength between IL and tocopherol was weakened by the solvation, the order of interaction strength of different IL–tocopherol complexes was not affected. For both kinds of tocopherol homologs, the interaction energy with [bmim]Cl was higher than that with [bmim]BF_4, and for both kinds of ILs, the interaction energy with δ-tocopherol was higher than that with α-tocopherol. In the second strategy, the optimized gas-phase structures were further optimized within the implicit solvent before the interaction energy was calculated. The results (Table 6) showed that the order of interaction strength was still in accordance with that in gas phase, except that the interaction energy of [bmim]BF_4-α-tocopherol was a little higher than that of [bmim]Cl-α-tocopherol. It should be noted that the Gaussian 03 software could not incorporate the ionic strength information of the implicit solvent when it is running a geometry optimization, thus this exception probably stems from the inherent inaccuracy of the calculation rather than the solvation effect.

As the implicit solvation approach using PCM has several notable deficiencies, as mentioned by the above results and previous literature,[58] the solvation effect was also investigated by the second approach, using the COSMO-RS.[59] COSMO-RS introduces the vivid concept of polarization charge density (σ) profiles for a qualitative and quantitative comparison of the polarity distribution on molecular surfaces, which integrates the description of electrostatic, hydrogen bonding, and hydrophobicity of a structure. Importantly, this methodology provides a direct quantitative scaling of the thermodynamic properties of solvents in a specific solvation environment, and the specific solvent–solute interactions determining the solubility of solutes can be quantitatively discussed through force field analysis of the measures derived from COSMO-RS computation.[60] Table 7 lists the three descriptor parameters for the energies contributions to the solvation interactions of tocopherols with ILs: H_{MF} (misfit interaction energy), H_{HB} (hydrogen-bonding interaction energy), and H_{VDW} (van der Waals interaction energy). It is

Table 5. Second-Order Stabilization Energy $E^{(2)}$ from NBO Analysis and the Composition of Donor/Acceptor NBOs of [bmim]Cl-Tocopherol Complex at B3LYP/6-31+G (d,p) Level

Donor	Donor Composition	Acceptor	Acceptor Composition	$E^{(2)}$ (kcal mol^{-1})
[bmim]Cl-α-tocopherol				
BD (2) C_{29}—C_{33}	$0.71(sp^{99.99}d^{2.44})_C + 0.71(sp^{1.00})_C$	BD* (1) C_7—H_{14}	$0.60(sp^{2.72})_C - 0.80(s)_H$	0.56
BD (2) C_{36}—C_{38}	$0.70(sp^{1.00})_C + 0.72(sp^{1.00})_C$	BD* (1) C_7—H_{14}	$0.60(sp^{2.72})_C - 0.80(s)_H$	0.24
[bmim]Cl-γ-tocopherol				
BD (2) C_{32}—C_{34}	$0.69(sp^{1.00})_C + 0.72(sp^{1.00})_C$	BD* (1) C_7—H_{14}	$0.60(sp^{2.78})_C - 0.80(s)_H$	0.10
LP (2) O_{35}	0.01% s + 99.91% p + 0.09% d	BD* (2) N_1—C_5	$0.53(sp^{99.99}d^{2.37})_N - 0.85(sp^{99.99}d^{15.78})_C$	0.09
[bmim]Cl-δ-tocopherol				
LP (2) O_{39}	0.11% s + 99.79% p + 0.09% d	BD* (2) N_1—C_5	$0.53(sp^{99.99}d^{2.70})_N - 0.84(sp^{99.99}d^{9.72})_C$	0.18

Table 6. BSSE-Corrected Interaction Energy ΔE of IL–Tocopherol Complex at B3LYP/6-31+G (d,p) Level with PCM Solvation Model* (kJ mol^{-1})

	Single-point calculation		Optimized with solvation	
IL	α-Tocopherol	δ-Tocopherol	α-Tocopherol	δ-Tocopherol
[bmim]BF_4	−1.05	−8.48	−6.42	−9.42
[bmim]Cl	−5.29	−13.61	−4.64	−12.10

*The gas-phase BSSE energy of the solvated geometry was used to perform the BSSE correction.

noted that the H_{MF} and H_{VDW} values for different complexes are quite close to each other, and the major difference in the energy contributions of different IL–tocopherol interactions is the H_{HB}, clearly indicating the important role of hydrogen-bonding interaction in the solvation of tocopherols in ILs. Furthermore, the strength of hydrogen-bonding interaction follows the order [bmim]Cl > [bmim]BF_4 for different ILs and δ-tocopherol > α-tocopherol for different tocopherols, which are well consistent with the results in gas-phase calculation and experiments. Combining the results of both PCM calculation and COSMO-RS calculation, the correlation between the IL–tocopherol hydrogen-bonding interaction and the extractive separation of tocopherols by ILs was considered not to be modified by the solvation effect, although the interaction strength was weakened. Correspondingly, the reliability of this correlation is considered increased.

Amino acid and acetate ILs as extractant: calculation and experiment

Amino acid ILs whose anions are the conjugate base of amino acids have attracted much attention as alternative solvent in capturing carbon dioxide and have also been used for extracting phenolic compounds from esters.[13,61,62] Nevertheless, the potential of amino acid ILs as extractant for separating phenolic homologs has not been evaluated. The discussion earlier has exhibited the feasibility of the used quantum chemical calculation method in predicting the experimental results of separating tocopherol homologs by IL-mediated extraction. Thus, similar theoretical calculations were performed on the interaction between 1-ethyl-3-methylimidazolium glycine ([emim]Gly) and tocopherols, to prognosis the feasibility of amino acid ILs as novel extractant for separating tocopherol homologs before experiments. Electrostatic potential analysis on the optimized structure of [emim]Gly ion pair shows that there are two types of negative region (Figure 8), one near the amino group and the other near the carboxyl group. Correspondingly, two kinds of stable structures were obtained for [emim]Gly-tocopherol complex where the phenolic hydroxyl group lies either near the amino group or near the carboxyl group, nevertheless, the latter was found more stable. Geometry, AIM, and NBO analysis on the optimized geometry of [emim]Gly-tocopherol complex (Figure 9) exhibits that there are hydrogen-bonding

Table 7. COSMO-RS Derived Energies Contributions to the Solvation Interactions of Tocopherols with ILs (kJ mol^{-1})

	α-Tocopherol			δ-Tocopherol		
IL	H_{MF}	H_{HB}	H_{VDW}	H_{MF}	H_{HB}	H_{VDW}
[bmim]BF_4	34.0	−3.8	−98.2	32.1	−6.7	−92.3
[bmim]Cl	32.9	−10.0	−103.9	30.7	−18.0	−97.9

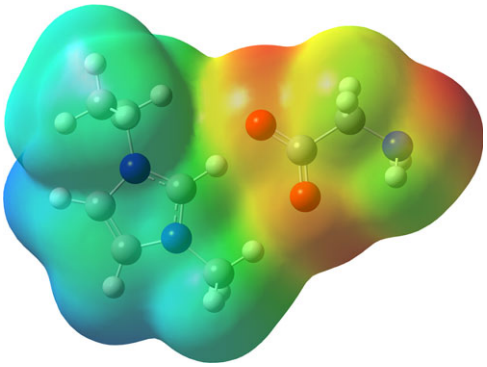

Figure 8. B3LYP/6-31+G(d,p) electrostatic potential mapped onto the 0.0004 density isosurface (unit: electron bohr^{-3}) for the optimized structures of [emim]Gly.

The scale spans −46.4 (red) through 0.0 (green) to 46.4 (blue) (unit: kcal mol^{-1}). [Color figure can be viewed in the online issue, which is available at wileyonlinelibrary.com.]

interactions between [emim]Gly and tocopherol, not only between the phenolic hydrogen atom of tocopherol and the carboxyl oxygen atom of anion but also between the phenolic oxygen atom of tocopherol and the alkyl hydrogen atom of cation (Table 8). The sum of ρ_c of $O_{anion}\cdots H_{O-H}$ and $O_{O-H}\cdots H_{C-H}$ in [emim]Gly-α-tocopherol complex is 0.0632 au, much higher than that of $Cl\cdots H_{O-H}$ in [bmim]Cl-α-tocopherol. The sum of $E^{(2)}$ of LP $O_{anion}\cdots$BD* H_{O-H} and LP $O_{O-H}\cdots$BD* H_{C-H} donor–acceptor interactions is 37.47 kcal mol^{-1}, much higher than that of LP Cl–BD* $H_{O-H.}$ The interaction energy of [emim]Gly-α-tocopherol, 49.77 kJ mol^{-1}, is also higher than that of [bmim]Cl-α-tocopherol. The comparison of calculation results between [emim]Gly-δ-tocopherol and [bmim]Cl-δ-tocopherol leads to the same results. In brief, the corresponding ρ_c, $E^{(2)}$, and ΔE quantities of [emim]Gly-tocopherol complex are all much higher than the [bmim]Cl-tocopherol analog, so the hydrogen-bonding interaction of [emim]Gly with tocopherol is much stronger than that of [bmim]Cl, implying that notably higher distribution coefficients of tocopherols would be obtained if [emim]Gly is used as extractants instead of [bmim]Cl, [bmim]Br, and [bmim]BF_4. Besides, the ρ_c, $E^{(2)}$, and ΔE values of [emim]Gly-δ-tocopherol are higher than those of [emim]Gly-α-tocopherol, which is in accordance with the results obtained for [bmim]Cl and other two ILs, indicating that [emim]Gly could selectively interact with different tocopherol homologs and probably bring on higher distribution coefficient of δ-tocopherol than α-tocopherol. It should be noted that the ρ_c and $\nabla^2\rho_c$ values of $O_{anion}\cdots H_{O-H}$ in [emim]Gly-tocopherol complexes from AIM analysis are higher than the proposed upper limit for hydrogen bonds in the Popelier's criteria. Nevertheless, based on the agreement to other AIM criteria proposed by Popelier and the information obtained from geometry and NBO analysis, the interaction between carboxyl oxygen atom and phenolic hydroxyl in [emim]Gly-tocopherol complex is still identified as hydrogen bond, but which is stronger than common hydrogen bonds including those between tocopherol and [bmim]Cl or the other two ILs.

The quantum chemical calculation results indicates that [emim]Gly is likely to be a more efficient extractant for separating tocopherol homologs than the previously utilized ILs.

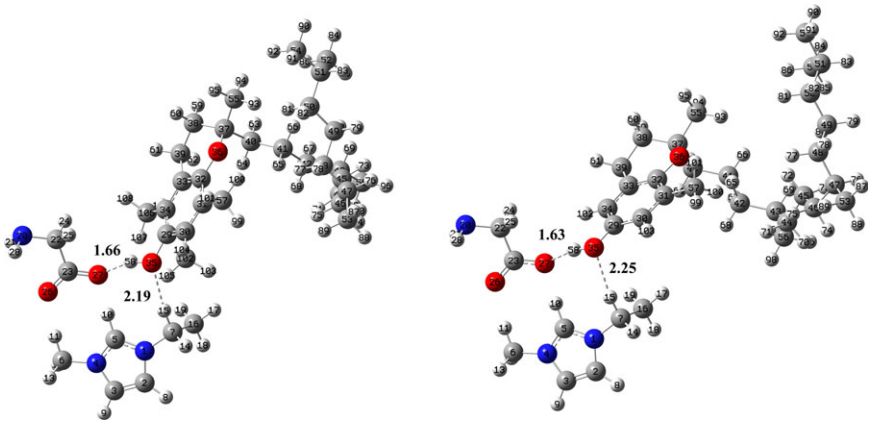

Figure 9. Optimized structure of [emim]Gly-α-tocopherol (left) and [emim]Gly-δ-tocopherol (right) complexes at B3LYP/6-31+G(d,p) level.

Dashed lines imply hydrogen bonds, with decimals showing the distances (unit: Å). [Color figure can be viewed in the online issue, which is available at wileyonlinelibrary.com.]

This speculation was confirmed by extraction experiments in this work. As presented in Table 3, it is found that the distribution coefficients of tocopherols obtained with [emim]Gly are much higher than those with other ILs. The distribution coefficient of δ-tocopherol is 19.2 with [emim]Gly, about five times higher than that with [bmim]Cl, sixteen times than that with [bmim]Br, and sixty-four times than that with [bmim]BF_4. Furthermore, the distribution coefficients are in the order δ-tocopherol > γ-tocopherol > α-tocopherol. The ratios of the distribution coefficient of δ-/γ-tocopherol to that of α-tocopherol, namely, selectivity, are a little higher than that using [bmim]Cl as extractant and much higher than those using [bmim]Br and [bmim]BF_4.

Glycine is just one of the various amino acids that can serve as the anion source, and it would be interesting to see the predictive ability of the used approach for different amino acid anions. In this work, an attempt has been made for [emim]Gly and [emim]Ala whose molecular structures are very similar except for one methyl group (see Supporting Information, Figure S1). The DFT calculations showed that both the interaction sites and the interaction strength of [emim]Ala-tocopherol complexes were very similar to the [emim]Gly-tocopherol complexes (Table 8, Supporting Information, Figure S2), so it was expected that the extraction efficiency using [emim]Ala as extractant should be similar to that using [emim]Gly. As expected, the extraction experiments showed that the distribution coefficients and selectivities of tocopherols using [emim]Ala as extractant were indeed similar to those using [emim]Gly (Table 3). Although much more work is required for a comprehensive investigation on different amino acids due to their structural and property diversity, the above results could still be considered as a positive support to the predictive capability of the used method.

It was noted that the amino acid ILs have multiple hydrogen-bond acceptor sites, both amino nitrogen atom and carboxyl oxygen atoms. Therefore, it would also be interesting to see how the multiplicity affects the extraction efficiency. Compared to the [emim]Gly, there is an absence of primary amino group in the molecular structure of 1-ethyl-3-methylimidazolium acetate ([emim]Ac, see Supporting Information, Figure S1). Nevertheless, it was found that the extraction efficiency of tocopherols using [emim]Ac as extractant was quite similar to that using [emim]Gly (Table 3). Furthermore, the DFT calculation also exhibited similar results for both the [emim]Ac and the [emim]Gly on the major interaction sites and strength (see Supporting Information, Figure S3). Thus, these results demonstrated that the amino group of amino acid ILs probably just played a rather secondary role in the extraction of tocopherols. And then, it also implied that the study on the hydrogen-bonding interaction between the phenolic hydroxyl group and the major acceptor

Table 8. Charge Density ρ_c, Its Laplacian $\nabla^2\rho_c$, and Energy Density H_c at the BCP from AIM Analysis, Second-Order Stabilization Energy $E^{(2)}$ from NBO Analysis, and the BSSE-Corrected Interaction Energy ΔE of [emim]Gly/[emim]Ala/[emim]Ac-Tocopherol Complex at B3LYP/6-31 + G (d,p) Level

Complex	BCP	$\rho_c \times 10^2$ (au)	$\nabla^2\rho_c \times 10^2$ (au)	$H_c \times 10^3$ (au)	Electron Delocalization	$E^{(2)}$ (kcal mol^{-1})	ΔE (kJ mol^{-1})
[emim]Gly-α-Tocopherol	$O_{27}\cdots H_{58}$	4.67	14.4	−0.3	LP O_{27}–BD* O_{35}—H_{58}	30.65	−49.77
	$O_{35}\cdots H_{15}$	1.65	4.70	−0.2	LP O_{35}–BD* C_7—H_{15}	6.82	
[emim]Gly-δ-Tocopherol	$O_{27}\cdots H_{58}$	5.03	15.1	−1.2	LP O_{27}–BD* O_{35}—H_{58}	34.57	−57.62
	$O_{35}\cdots H_{15}$	1.54	4.21	−0.3	LP O_{35}–BD* C_7—H_{15}	5.30	
[emim]Ala-α-Tocopherol	$O_{29}\cdots H_{61}$	4.72	14.6	−0.3	LP O_{29}–BD* O_{38}—H_{61}	31.00	−48.68
	$O_{38}\cdots H_{15}$	1.66	4.74	−0.2	LP O_{38}–BD* C_7—H_{15}	6.94	
[emim]Ala-δ-Tocopherol	$O_{29}\cdots H_{61}$	5.09	15.3	−1.4	LP O_{29}–BD* O_{38}—H_{61}	35.66	−56.93
	$O_{38}\cdots H_{15}$	1.48	4.08	−0.2	LP O_{38}–BD* C_7—H_{15}	5.16	
[emim]Ac-α-Tocopherol	$O_{106}\cdots H_{30}$	4.99	15.0	−1.1	LP O_{106}–BD* O_7—H_{30}	33.95	−51.19
	$O_7\cdots H_{96}$	1.59	4.61	−0.1	LP O_7–BD* C_{88}—H_{96}	4.84	
[emim]Ac-δ-Tocopherol	$O_{25}\cdots H_{56}$	5.27	15.5	−2.0	LP O_{25}–BD* C_{33}—H_{56}	36.54	−59.12
	$O_{33}\cdots H_{15}$	1.47	4.06	−0.2	LP O_{33}–BD* C_7—H_{15}	5.10	

site could give valuable information about the extraction mechanism and benefit the prediction of extraction efficiency. By the way, as the case of [emim]Gly, the calculated interaction strength of [emim]Ala/[emim]Ac with δ-tocopherol was stronger than that with α-tocopherol. This is consistent with the order of distribution coefficients of different tocopherol homologs in extraction experiments, indicating the ability of calculation results for interpreting the selectivity again.

Overall, the quantum chemical calculations in this work shows that intermolecular hydrogen-bonding interaction could be an important mechanism in the extraction of phenolic compounds or even isolating their homologs. ILs have relatively strong hydrogen-bond basicity, and the strength of basicity could be adjusted by the variation of cations and anions, so ILs could perform as favorable extractant in extracting phenolic compounds and separating phenolic homologs. The accordance of calculation results with experimental outcomes on IL-mediated extractive separation of tocopherol homologs, a model of phenolic homologs, has given an illustration of this point. Besides, the feasibility of quantum chemical calculation method used in this work in developing novel IL-type extractant is also revealed.

Conclusion

The essential role of hydrogen-bonding interaction in the extractive separation of phenolic compounds by IL-mediated extraction has been illustrated at the molecular level, through the theoretical calculations on the intermolecular interaction of IL with the model compounds, tocopherols. Multiple analyses including geometry, AIM, NBO, and energy on the optimized structures of IL–tocopherol complexes demonstrate the importance of hydrogen bonds in the IL–tocopherol interactions. Furthermore, the charge density at the BCP, ρ_c, from AIM analysis, the second-order stabilization energy, $E^{(2)}$, from NBO analysis, and the BSSE-corrected interaction energy, ΔE, of IL–tocopherol complex all exhibit that the strength of intermolecular hydrogen bonds is in the order [emim]Gly/[emim]Ala/[emim]Ac $>$ [bmim]Cl $>$ [bmim]Br $>$ [bmim]BF_4 for different ILs and δ-tocopherol $>$ γ-tocopherol $>$ α-tocopherol for different tocopherol homologs, which was in good accordance with the experimental distribution equilibrium of tocopherols in IL-mediated liquid–liquid extraction. The solvation effect could weaken the interaction strength, but the order of relative strength of different ILs/tocopherols and the correlation between hydrogen-bonding interaction and extraction efficiency still held. The anion-hydroxyl intermolecular hydrogen bonds in IL–tocopherol complexes are relatively strong compared to common hydrogen bonds. Their total energy densities at BCP, H_c, are all smaller than zero, reflecting their partially covalent nature. Especially, the intermolecular hydrogen bond $O_{anion}\cdots H_{O-H}$ in [emim]Gly/[emim]Ala/[emim]Ac-tocopherol complex is so strong that its ρ_c value is higher than the proposed upper limit for hydrogen bonds in Popelier's criteria. The performed theoretical calculations facilitate the development of novel IL extractants. More efficient extractant for tocopherols separation, [emim]Gly and [emim]Ala, have been developed through a theoretical prognosis and an experimental verification. The distribution coefficients of tocopherols obtained with [emim]Gly or [emim]Ala as extractant were at least five times higher than those obtained with three previously used ILs. The comparative study on [emim]Ac and [emim]Gly demonstrated the dominant role of carboxyl terminal of amino acid ILs in their hydrogen-bonding interaction with tocopherols, and it indicated that the theoretical study on the interaction between the phenolic hydroxyl and the major hydrogen-bond acceptor site of IL could be able to give a reasonable interpretation of the extraction efficiency of ILs. At last, it is expected that the results of this work will be also helpful for understanding and improving the extraction of other phenolic compounds by ILs.

Acknowledgments

The authors are grateful for the financial supports from National Natural Science Foundation of China (20936005, 21106127, and 21222601). Besides, the authors gratefully acknowledge Prof. Haoran Li at Department of Chemistry, Zhejiang University, China for providing the Gaussian 03 program and helpful guidance.

Literature Cited

1. Han X, Armstrong DW. Ionic liquids in separations. *Acc Chem Res*. 2007;40:1079–1086.
2. Poole CF, Poole SK. Extraction of organic compounds with room temperature ionic liquids. *J Chromatogr A*. 2010;1217:2268–2286.
3. Manic MS, Najdanovic-Visak V, Da Ponte MN, Visak ZP. Extraction of free fatty acids from soybean oil using ionic liquids or poly (ethyleneglycol)s. *AIChE J*. 2011;57:1344–1355.
4. Hernández-Fernández FJ, de Los Ríos AP, Gómez D, Rubio M, Víllora G. Selective extraction of organic compounds from transesterification reaction mixtures by using ionic liquids. *AIChE J*. 2010;56:1213–1217.
5. Pereiro AB, Rodríguez A. An ionic liquid proposed as solvent in aromatic hydrocarbon separation by liquid extraction. *AIChE J*. 2010;56:381–386.
6. Patnaik P. *Handbook of Environmental Analysis: Chemical Pollutants in Air, Water, Soil, and Solid Wastes*, 2nd ed. Boca Raton, FL, USA: CRC Press, Taylor & Francis Group, 2009.
7. Liu ZG. *Food Nutriology*. Beijing, PR China: China Light Industry Press, 1991.
8. Egorov VM, Smirnova SV, Pletnev IV. Highly efficient extraction of phenols and aromatic amines into novel ionic liquids incorporating quaternary ammonium cation. *Sep Purif Technol*. 2008;63:710–715.
9. Visser AE, Swatloski RP, Rogers RD. PH-dependent partitioning in room temperature ionic liquids provides a link to traditional solvent extraction behavior. *Green Chem*. 2000;2:1–4.
10. Fan J, Fan YC, Pei YC, Wu K, Wang JJ, Fan MH. Solvent extraction of selected endocrine-disrupting phenols using ionic liquids. *Sep Purif Technol*. 2008;61:324–331.
11. Khachatryan KS, Smirnova SV, Torocheshnikova II, Shvedene NV, Formanovsky AA, Pletnev IV. Solvent extraction and extraction-voltammetric determination of phenols using room temperature ionic liquid. *Anal Bioanal Chem*. 2005;381:464–470.
12. Bekou E, Dionysiou DD, Qian RY, Botsaris GD. Extraction of chlorophenols from water using room temperature ionic liquids. *ACS Symp Ser*. 2003;856:544–560.
13. Li M, Pham PJ, Pittman CU, Li T. Selective solid-phase extraction of α-tocopherol by functionalized ionic liquid-modified mesoporous SBA-15 adsorbent. *Anal Sci*. 2008;24:1245–1250.
14. Katsuta S, Nakamura K, Kudo Y, Takeda Y. Mechanisms and rules of anion partition into ionic liquids: phenolate ions in ionic liquid/water biphasic systems. *J Phys Chem B*. 2012;116:852–859.
15. Kumar L, Banerjee T, Mohanty K. Prediction of selective extraction of cresols from aqueous solutions by ionic liquids using theoretical approach. *Sep Sci Technol*. 2011;46:2075–2087.
16. Colegate SM, Molyneux RJ. *Bioactive Natural Products: Detection, Isolation, and Structural Determination*, 2nd ed. Boca Raton, FL, USA: CRC Press, Taylor & Francis Group, 2008.
17. Sticher O. Natural product isolation. *Nat Prod Rep*. 2008;25:517–554.
18. Packer L. Protective role of vitamin E in biological systems. *Am J Clin Nutr*. 1984;53:1050–1055.
19. Yang Q, Xing H, Su B, Yu K, Bao Z, Yang Y, Ren Q. Improved separation efficiency using ionic liquid-cosolvent mixtures as the extractant in liquid–liquid extraction: a multiple adjustment and synergistic effect. *Chem Eng J*. 2012;181–182:334–342.

20. Yang QW, Xing HB, Cao YF, Su BG, Yang YW, Ren QL. Selective separation of tocopherol homologues by liquid–liquid extraction using ionic liquids. *Ind Eng Chem Res*. 2009;48:6417–6422.
21. Anderson JL, Ding J, Welton T, Armstrong DW. Characterizing ionic liquids on the basis of multiple solvation interactions. *J Am Chem Soc*. 2002;124:14247–14254.
22. Frisch MJ, Trucks GW, Schlegel HB, Scuseria GE, Robb MA, Cheeseman JR, Zakrzewski VG, Montgomery JA, Stratmann RE, Burant JC, Dapprich S, Millam JM, Daniels AD, Kudin KN, Strain MC, Farkas O, Tomasi J, Barone V, Cossi M, Cammi R, Mennucci B, Pomelli C, Adamo C, Clifford S, Ochterski J, Petersson GA, Ayala PY, Cui Q, Morokuma K, Malick DK, Rabuck AD, Raghavachari K, Foresman JB, Cioslowski J, Ortiz JV, Stefanov BB, Liu G, Liashenko A, Piskorz P, Komaromi I, Gomperts R, Martin RL, Fox DJ, Keith T, Al-Laham MA, Peng CY, Nanayakkara A, Gonzalez C, Challacombe M, Gill PMW, Johnson B, Chen W, Wong MW, Andres JL, Gonzalez C, Head-Gordon ME, Replogle S, Pople JA. *Gaussian 03*. Pittsburgh, PA: Gaussian, Inc., 2003.
23. Lee CT, Yang WT, Parr RG. Development of the Colle-Salvetti correlation-energy formula into a functional of the electron-density. *Phys Rev B*. 1988;37:785–789.
24. Becke AD. Density–functional thermochemistry. III. The role of exact exchange. *J Chem Phys*. 1993;98:5648–5652.
25. *Chem3D Ultra 10.0, ChemOffice Ultra, 2006*. Cambridge, MA, USA: CambridgeSoft Corporation, 2006.
26. Bader RFW. *Atoms in Molecules: A Quantum Theory*. Oxford, UK: Oxford University Press, 1990.
27. Popelier PL. *Atoms in Molecules: An Introduction*. Harlow, UK: Prentice-Hall, 2000.
28. Stone AJ, Alderton M. Distributed multipole analysis—methods and applications. *Mol Phys*. 1985;56:1047–1064.
29. Reed AE, Curtiss LA, Weinhold F. Intermolecular interactions from a natural bond orbital donor–acceptor viewpoint. *Chem Rev*. 1988;88:899–926.
30. Keith TA. *AIMAll, Version 10.03.25*. Overland Park, KS, USA: TK Gristmill Software, 2010.
31. Boys SF, Bernardi F. Calculation of small molecular interactions by differences of separate total energies—some procedures with reduced errors. *Mol Phys*. 1970;19:553–566.
32. Cances E, Mennucci B, Tomasi J. A new integral equation formalism for the polarizable continuum model: theoretical background and applications to isotropic and anisotropic dielectrics. *J Chem Phys*. 1997;107:3032–3041.
33. Singh T, Kumar A. Static dielectric constant of room temperature ionic liquids: internal pressure and cohesive energy density approach. *J Phys Chem B*. 2008;112:12968–12972.
34. Stearn AE, Eyring H. The deduction of reaction mechanisms from the theory of absolute rates. *J Chem Phys*. 1937;5:113–124.
35. *COSMOthermX, Version c3.0, Release 12.01*. Leverkusen, Germany: COSMOlogic GmbH & Co. KG, 2011.
36. TURBOMOLE V6.3 2012, a development of University of Karlsruhe and Forschungszentrum Karlsruhe GmbH, 1989–2007, TURBOMOLE GmbH, since 2007, 2011. Available at: http://www.turbomole.com.
37. Schafer A, Huber C, Ahlrichs R. Fully optimized contracted gaussian-basis sets of triple zeta valence quality for atoms Li to Kr. *J Chem Phys*. 1994;100:5829–5835.
38. Becke AD. Density-functional exchange-energy approximation with correct asymptotic-behavior. *Phys Rev A*. 1988;38:3098–3100.
39. Perdew JP. Density-functional approximation for the correlation-energy of the inhomogeneous electron-gas. *Phys Rev B*. 1986;33:8822–8824.
40. Ohno H, Fukumoto K. Amino acid ionic liquids. *Acc Chem Res*. 2007;40:1122–1129.
41. Fukumoto K, Yoshizawa M, Ohno H. Room temperature ionic liquids from 20 natural amino acids. *J Am Chem Soc*. 2005;127:2398–2399.
42. Platts JA. Theoretical prediction of hydrogen bond donor capacity. *Phys Chem Chem Phys*. 2000;2:973–980.
43. Hunt PA, Gould IR, Kirchner B. The structure of imidazolium-based ionic liquids: insights from ion-pair interactions. *Aust J Chem*. 2007;60:9–14.
44. Turner EA, Pye CC, Singer RD. Use of ab initio calculations toward the rational design of room temperature ionic liquids. *J Phys Chem A*. 2003;107:2277–2288.
45. Economou IG, Karakatsani EK, Logotheti GE, Ramos J, Vanin AA. Multi-scale modeling of structure, dynamic and thermodynamic properties of imidazolium-based ionic liquids: ab initio DFT calculations, molecular simulation and equation of state predictions. *Oil Gas Sci Technol*. 2008;63:283–293.
46. Dong K, Zhang S, Wang D, Yao X. Hydrogen bonds in imidazolium ionic liquids. *J Phys Chem A*. 2006;110:9775–9782.
47. Bondi A. Van der Waals volumes + radii. *J Phys Chem*. 1964;68:441–451.
48. Popelier P. Characterization of a dihydrogen bond on the basis of the electron density. *J Phys Chem A*. 1998;102:1873–1878.
49. Koch U, Popelier P. Characterization of C—H—O hydrogen-bonds on the basis of the charge-density. *J Phys Chem*. 1995;99:9747–9754.
50. Dhumal NR, Kim HJ, Kiefer J. Electronic structure and normal vibrations of the 1-ethyl-3-methylimidazolium ethyl sulfate ion pair. *J Phys Chem A*. 2011;115:3551–3558.
51. Mou Z, Li P, Bu Y, Wang W, Shi J, Song R. Investigations of coupling characters in ionic liquids formed between the 1-ethyl-3-methylimidazolium cation and the glycine anion. *J Phys Chem B*. 2008;112:5088–5097.
52. Arnold WD, Oldfield E. The chemical nature of hydrogen bonding in proteins via NMR: *J*-couplings, chemical shifts, and AIM theory. *J Am Chem Soc*. 2000;122:12835–12841.
53. Kaur D, Kohli R, Kaur RP. A comparative study on hydrogen bonding ability of thioformohydroxamic acid and formohydroxamic acid. *J Mol Struct: Theochem*. 2008;864:72–79.
54. Parveen S, Chandra AK, Zeegers-Huyskens T. Theoretical investigation of the hydrogen bonding interaction between substituted phenols and simple *O*- and *N*-bases. *J Mol Struct*. 2010;977:258–265.
55. Payal RS, Bharath R, Periyasamy G, Balasubramanian S. Density functional theory investigations on the structure and dissolution mechanisms for cellobiose and xylan in an ionic liquid: gas phase and cluster calculations. *J Phys Chem B*. 2012;116:833–840.
56. Du HB, Qian XH. The effects of acetate anion on cellulose dissolution and reaction in imidazolium ionic liquids. *Carbohydr Res*. 2011;346:1985–1990.
57. Riley KE, Vondrasek J, Hobza P. Performance of the DFT-D method, paired with the PCM implicit solvation model, for the computation of interaction energies of solvated complexes of biological interest. *Phys Chem Chem Phys*. 2007;9:5555–5560.
58. Klamt A. The COSMO and COSMO-RS solvation models. *Wiley Interdiscip Rev-Comput Mol Sci*. 2011;1:699–709.
59. Klamt A. Conductor-like screening model for real solvents: a new approach to the quantitative calculation of solvation phenomena. *J Phys Chem*. 1995;99:2224–2235.
60. Guo Z, Lue BM, Thomasen K, Meyer AS, Xu XB. Predictions of flavonoid solubility in ionic liquids by COSMO-RS: experimental verification, structural elucidation, and solvation characterization. *Green Chem*. 2007;9:1362–1373.
61. Gurkan BE, de la Fuente JC, Mindrup EM, Ficke LE, Goodrich BF, Price EA, Schneider WF, Brennecke JF. Equimolar CO2 absorption by anion-functionalized ionic liquids. *J Am Chem Soc*. 2010;132:2116–2117.
62. Goodrich BF, de la Fuente JC, Gurkan BE, Zadigian DJ, Price EA, Huang Y, Brennecke JF. Experimental measurements of amine-functionalized anion-tethered ionic liquids with carbon dioxide. *Ind Eng Chem Res*. 2011;50:111–118.

Manuscript received Mar. 13, 2012, and revision received Sep. 23, 2012.